Chemical Engineering Journal 113 (2005) 73–82

Chemical Engineering Journal

www.elsevier.com/locate/cej

Solid particle distribution of moderately concentrated suspensions in a pilot plant stirred vessel

M. Špidla *, V. Sinevič, M. Jahoda, V. Machoň

Department of Chemical Engineering, Institute of Chemical Technology, Technická 3, 166 28 Prague 6, Czech Republic

Received 19 March 2005; received in revised form 2 August 2005; accepted 23 August 2005

Abstract

Detailed particle distribution of a solid–liquid suspension in the just suspended state was measured by means of a conductivity probe. A total of eight experimental settings were investigated, involving two particle diameters (0.14 and 0.35 mm), two average particle concentrations (5 and 10 vol.%) and two impeller off-bottom clearances ($H_2/d = 1$ and 0.5). A pilot plant stirred vessel of 1 m in diameter stirred with flat six pitched-blade turbine was used. A particle-filled layer of suspension was observed in all these experiments, and was particularly pronounced at the solid concentration of 10 vol.% and impeller off-bottom clearance $H_2/d = 0.5$. The local solid concentration profiles within this layer were investigated. The axial and radial concentration gradients and their standard deviations were determined.

The results indicate the presence of a concentration gradient in the radial direction within the particle layer, and of significant concentration fluctuations at the interface between the particle layer and the clear liquid layer in the upper part of the stirred vessel.

Keywords: Mixing of suspensions; Pilot plant stirred vessel; Just suspended conditions; Local solids concentration; Axial-flow impeller

1. Introduction

Mechanical mixing is a common unit operation in chemical technology processes, biochemical industries, mineral processing industries and numerous other applications. The suspension of solid particles in a liquid is encountered, e.g. in leaching, reactions utilising a solid catalyst, crystallisation, coagulation, and water treatment. In the course of mixing, the solid particles are moving in the liquid phase and thereby increase the rate of mass and/or heat transfer between the particles and the liquid. In accordance with operational demands, it is possible to conduct the mixing of suspension either in the state of complete suspension, when no particle remains at the vessel bottom for more than 1–2 s [1], or in the state of a homogeneous suspension, with the solid phase uniformly distributed in the stirred vessel. The latter case is difficult to attain and usually is not required in most industrial applications.

In the processes mentioned above, the knowledge of local solids concentration profiles in a mechanically agitated vessel is very important. Numerous methods are available for measuring local solids concentrations in a slurry in stirred vessels. Optical methods are very popular and much useful work has been done here; the Refs. [2–4] are an example. These non-intrusive methods are generally limited to solids concentrations less than 1–2%. This is due to the scattering and blocking of light by the solids between the source and the detector. Typical representatives of in situ concentration measurements are the sample withdrawal method and the conductivity probe measurements. The former method is the simplest one and has been employed, e.g. by MacTaggart et al. [5] and by Barresi et al. [6–8]. The samples of the suspension are taken from different locations in the vessel, and the solid phase concentration is determined. However, it is extremely difficult to obtain representative samples from a stirred vessel due to inertia differences between the fluid and the particles of different sizes or densities [5,9]. The conductivity measurement is based on the conductivity changes of the suspension depending on the quantity of solid particles present. Two-electrode conductivity probes were used e.g. in the works [10–14] and recently in [15,16]. Four-electrode conductivity sensors developed by Considine and Considine [17] and by Nasr-El-Din et al. [18] were used e.g. in their works [19,20]. The conductivity method has the advantage of requiring low investment and of lending itself to measurements in highly concentrated suspensions. On the other hand, its accuracy

* Corresponding author. Tel.: +420 2 20443233; fax: +420 2 3333 7335.
E-mail address: Michal.Spidla@vscht.cz (M. Špidla).

1385-8947/$ – see front matter © 2005 Elsevier B.V. All rights reserved.
doi:10.1016/j.cej.2005.08.005

Nomenclature

A	slope of the straight line, vol.%
b	baffle width, m
B	y-intercept of the straight line ($C_{V_{avg\,axial}}$ in the vessel axis), vol.%
C_V	local solids volume concentration, %
$C_{V_{avg}}$	average solids volume concentration, %
$C_{V_{avg\,axial}}$	average solids volume concentration in an axial direction, %
$C_{V_{std}}$	standard deviation of local solids volume concentration, %
d	impeller diameter, m
d_p	particle diameter, m
D	vessel diameter, m
Fr'	modified Froude number
g	acceleration of gravity, m s^{-2}
h	actual position of measuring point in axial direction (i.e. distance from vessel bottom), m
H	filling height, m
H_2	impeller off-bottom clearance, m
K_c	concentration calibration constant in Eq. (1)
n_{js}	just suspended agitation speed, rpm
r	actual position of measuring point in a radial direction, m
R	vessel radius, m
V	vessel volume, m^3
w	width of blades, m

Greek letters

γ_f	relative electric conductivity of liquid, S m^{-1}
γ_s	relative electric conductivity of suspension, S m^{-1}
ρ	density of liquid, kg m^{-3}
ρ_p	solids density, kg m^{-3}

of measurement is lower at solid phase concentrations below 3 vol.%, and there is an intrusive effect of the probe in the vessel. The influence of the probe on the suspension process can be eliminated by suitably adjusting the size proportions of the probe versus the experimental vessel.

The advantage of a two-electrode conductivity probe was employed and the moderately concentrated systems with 5 and 10 vol.% of the solid phase were investigated in this work. The pilot plant stirred vessel (D = 1 m) was used, in which the influence of the small probe on the pattern of hydrodynamic flow could be considered to be negligible. All experiments were performed under conditions corresponding to a full off-bottom lifting of solids, which closely relate to the just-suspended agitation speed, n_{js}. A clear liquid layer above a dense suspension was clearly observed under these experimental conditions. This phenomenon has frequently been observed in the past and was firstly discussed by Musil [21]. Further papers [4,22–31] describe the effects on this phenomenon of particle size and concentration, impeller type and speed, impeller off-bottom clearance, stirrer and vessel size, mixing time and physical properties of the system. Several references are indirect, focused on the study of various suspension system parameters, e.g. on the conditions of complete suspension. For example, the mixing time in systems where the particle suspension layer is observed may be longer by two or more orders of magnitude than in the single phase case [24]. The influence of stirrer type and clearance and of the solid size and concentration on the cloud height was studied e.g. by Barresi and Baldi [25]. The cloud height is lower when a pitched blade turbine is used instead of the Rushton turbine. The cloud height increases with stirrer speed and is lower with larger particles and at higher solid loading. A review of the particle suspension layer can be found in recent work by Micale et al. [31], dealing with CFD simulations of particle suspension height. It should be noted that the particle suspension layer may occur also in the three-phase (liquid–gas–solid) systems [26].

In all the works mentioned above, little attention was given to the solid particle distribution within the layer. Buurman et al. [22] studied a relatively homogeneous, highly concentrated particle layer. Under their test conditions, there were hardly any differences in the solids concentrations at three sample withdrawal points situated in an axial direction. Radial concentration profiles were not investigated in their work. The significance of the radial concentration gradient has never been analysed in detail, even though the presence of radial concentration gradient depends on the stirrer type and speed as well as on impeller off-bottom clearance, particle diameter and solid loading. Literature data suggest that generally, the radial concentration gradients are negligible [6,13,14,32,33]. However, this assumption cannot be generalised. Micheletti et al. [15] have obtained data at different radial positions indicating the presence of radial concentration gradients. These are generally minor for small particle sizes, but they increase significantly when particles of larger size or density are suspended. Angst and Kraume [34,35] determined axial and radial particle distributions using an endoscope system. In all cases, the measurements indicated a fairly homogeneous distribution of the dispersed phase below the stirrer. The local concentrations were close to the mean particle concentration. Above the stirrer an abatement of the dispersed phase concentration was determined near the impeller shaft. The reduction is increased with higher mean particle concentration, larger bottom distances and greater particle diameters.

The principal aim of this paper was to determine the particle distribution in one horizontal quadrant of the vessel volume. The particle distributions were determined at 15 points spaced at nine elevations above the vessel bottom. The points were situated on four vertical planes passing through the vessel axis and with four values of radii. Such a detailed measuring mesh made it possible to analyse in greater detail the radial concentration gradients.

2. Experimental

2.1. Local solid concentration measurements

A two-electrode conductivity probe measured the local concentrations of the solid particles, see Fig. 1. The outer (earthed) electrode was formed by six parallel rods of stainless steel placed

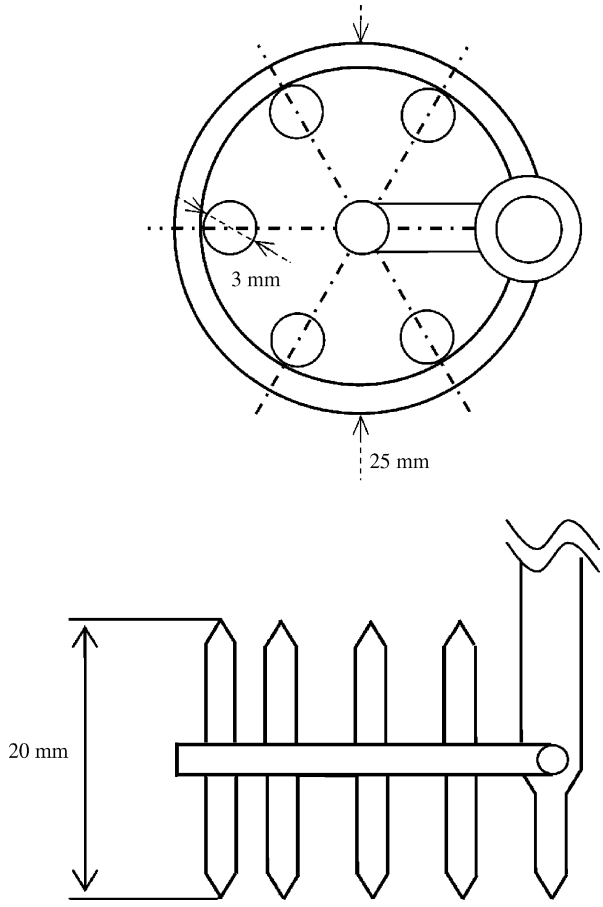

Fig. 1. Conductivity probe.

in the corners of a regular hexagon and conductively connected with a ring joined to a main carrying tube. The carrying tube was 150 cm long, so that the connector joining the probe with the conductivity device was sufficiently high above the liquid surface in the experimental vessel. The inner (measuring) electrode was made of a stainless steel rod placed in the centre of the ring. The volume of the measured space was 6.3 cm^3, compared with 7.85×10^5 cm^3 (i.e. 0.785 m^3) of the whole experimental vessel volume. In this case, the influence of the probe on the suspension process could be considered negligible.

The layout of the experimental apparatus is shown in Fig. 2. It consisted of the following parts:

- A flat-bottomed, cylindrical, transparent Plexiglas, pilot plant stirred vessel of a diameter $D = 1$ m equipped with four standard baffles, $b = 0.1D$ wide. The height of filling, H, in the vessel was equal to the vessel diameter, $H = D$.
- An opto-electronic disc system coupled with a digital counter was used for measuring the impeller speed. The accuracy of the impeller speed adjustment was ±1 rpm. The impeller shaft was driven by a servo-controlled variable-speed DC motor by means of a V-belt and a pulley.
- A conductivity measuring probe was connected to the conductivity meter input. The output voltage signal from this conductivity meter was connected to the analogue input of an AD converter, which was part of the computer-measuring

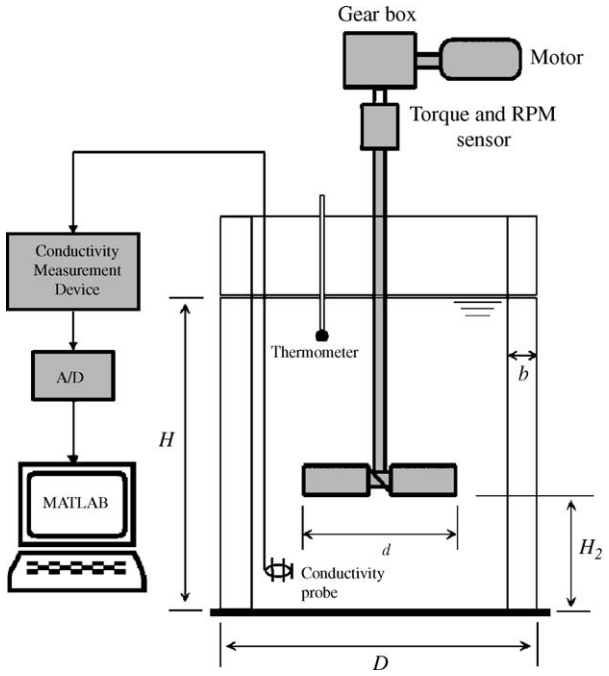

Fig. 2. Experimental apparatus.

card. Matlab software was used to sample the voltage values, which corresponded to the conductivity values of the suspension inside the probe.

In an earlier paper [11], a compensation sensor (a second conductivity probe) was used to eliminate the effects of temperature changes. In our experiments, a single conductivity probe was used and, instead of the compensation probe that would measure the conductivity of water γ_f, the effects of temperature were taken care of by temperature calibration of the probe. The advantage of temperature calibration consists in that it eliminates any effects whereby the two probes might electrically influence one another during the measurement. Moreover, due to slight differences in geometry the probes may have different temperature constants. The temperature calibration was undertaken in a thermostat and extended over the temperature range of 20–30°C, i.e. the range used in the experiments. A linear response was obtained. The temperature of water inside the vessel was measured during experiments, and the conductivity of water γ_f was simultaneously calculated from calibration. It should be noted that the temperature increase during one set of experiments was +0.2°C at maximum due to the large volume of liquid, giving rise to only a slight effect on the conductivity measurements. Before each set of experiments, both temperature and concentration calibrations were performed in the same tap water used in experiments, to eliminate any influence of different physical properties of water, e.g. different water salinity or bacterial contamination.

The concentration calibration used to calculate the volumetric concentration of solid particles followed the relation:

$$\frac{\gamma_s}{\gamma_f} = 1 - K_c C_V \quad (1)$$

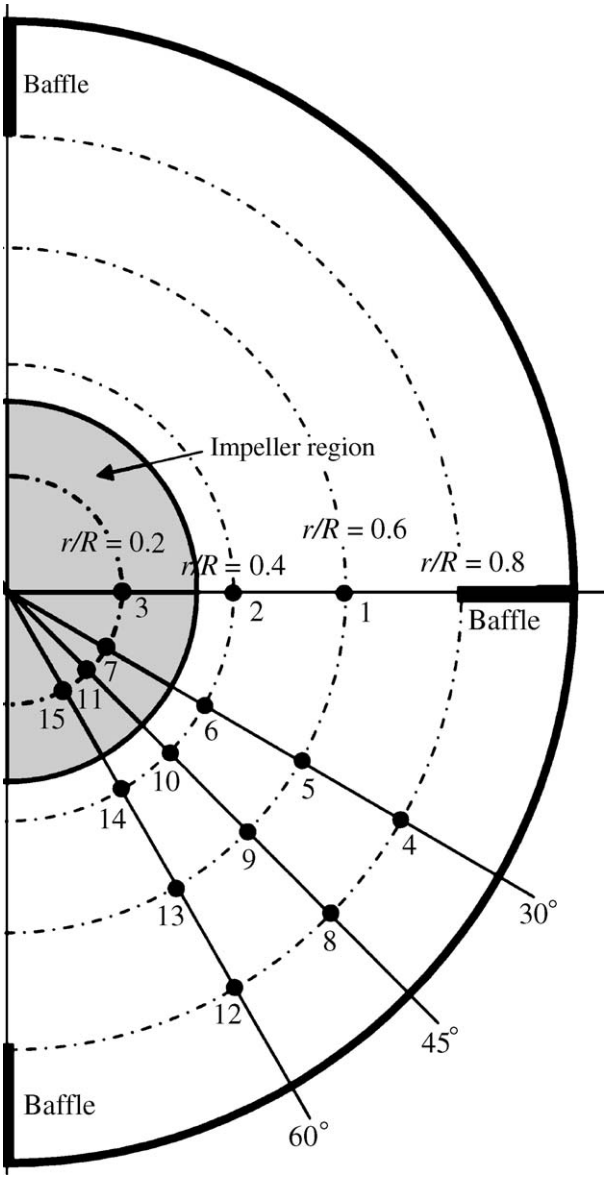

Fig. 3. Location of measuring points.

where K_c is the concentration calibration constant, γ_s the conductivity of solid–liquid suspension and C_V the local particle concentration. The concentration calibration was performed in a 200 mm diameter fluidized bed column. Machoň et al. [11] and Mak and Ruszkowski [14] obtained the same functional relationship between conductivity and solids concentration. The volumetric concentration measured in the settled particle bed was in the range of 0.60–0.63.

The locations of the measuring probe at a horizontal level are shown in Fig. 3. Assuming that the flow inside vertical quadrants of the vessel was symmetrical, only one quadrant of the vessel volume was investigated, i.e. the measurements proceeded in four vertical planes: the baffle plane and then in the planes inclined at 30°, 45° and 60° versus the baffle plane. The solids concentrations were measured at nine horizontal levels spaced vertically at 10 cm, thus covering the range extending from 10 to 90 cm from the vessel bottom. The total numbers of measuring points were 119 and 123 for the impeller off-bottom clearance $H_2/d = 1$ and for the clearance of 0.5, respectively. No measurements could be taken in the area under the impeller and at certain points at the elevation of 90 cm from the vessel bottom, because the upper end of the carrying tube of the probe reached too close to the motor (Nos. 3, 7, 11, 15). The accuracy of manual probe adjustment was ±0.2 cm in the axial and radial directions, and ±1° in the tangential direction. The impeller rotated in a clockwise direction.

2.2. Experimental conditions

The suspension of a classified ballotini in tap water was used as a model suspension, at the mean concentrations $C_{V_{avg}} = 5$ and 10 vol.% corresponding to 11.6 and 21.6 wt.%, respectively. The mean particle diameters were $d_p = 0.14$ and 0.35 mm and the particle densities were $\rho_p = 2478$ and 2500 kg m^{-3}, respectively. A flat six pitched-blade impeller (pitch angle 45°, blade width $w = 0.2d$) working in the pumping down regime was used. The vessel-to-impeller diameter ratio was $D/d = 3$ and the impeller off-bottom clearances were $H_2/d = 0.5$ and 1. The critical impeller speeds, n_{js}, corresponding to the full off-bottom suspension, were calculated from the correlation in Eq. (2):

$$Fr' = \frac{C_{41}e^{C_{42}C_V}\left(\frac{d_p}{D}\right)^{a_1+a_2C_V}}{\left\{1+\left[C_{31}e^{C_{32}C_V}\left(\frac{d_p}{D}\right)^{c_1+c_2C_V}\right]^{10}\right\}^{1/10}} \quad (2)$$

where d_p/D is the relative particle size and Fr' is the modified Froude number according to Eq. (3):

$$Fr' = \frac{n_{js}^2 d\rho}{g(\rho_p - \rho)} \quad (3)$$

The coefficients C_{41}, C_{42}, C_{31}, C_{32}, a_1, a_2, c_1 and c_2 are summarized in Table 1 and they are different for individual impeller types and off-bottom clearances. The coefficients were calculated from the experimental results obtained by us in the range of

Table 1
The regression coefficients in Eq. (2)

Variant A

H_2/d	C_{41}	C_{42}	a_1	a_2	C_{31}	C_{32}	c_1	c_2
1	8.442	51.951	0.455	5.671	5.293	44.607	0.270	5.766
0.5	5.982	55.500	0.468	6.216	12.914	35.213	0.406	4.292

Variant B

H_2/d	C_{41}	C_{42}	a_1	a_2
1	8.442	51.951	0.455	5.671
0.5	5.982	55.500	0.468	6.216
	C_{31}	C_{32}	c_1	c_2
1	5.293	44.607	0.270	5.766
0.5	12.914	35.213	0.406	4.292

Flat six pitched-blade impeller ($D/d = 3$), $H_2/d = 1$ and 0.5.

Table 2
Just suspended agitation speeds studied

Off-bottom clearance (H_2/d)	n_{js} (rpm)			
	$d_p = 0.14$ mm		$d_p = 0.35$ mm	
1	159	166	225	267
0.5	122	125	176	205

$d_p/D = 1.4 \times 10^{-4}$ to 3×10^{-3} and $C_{V_{avg}} = 2.5$–10 vol.% using the same impeller/vessel configuration. The theoretical background for deriving the Eq. (2) can be found in literature [36–40].

For the conditions tested, the just-suspended agitation speeds n_{js} are summarized in Table 2, and these were used in all the experiments. Visual observation confirmed the state of full suspension at these conditions.

3. Results and discussion

3.1. The data records

The presented axial concentration profiles are averaged values of the data records of time series obtained from four independent experiments performed on different days. This approach served to verify the reproducibility of experimental data. Three instantaneous concentration values were recorded during one experiment, and the recording of each of them took 30 s. During this period, ca. 250 values were taken for the calculation of the average local solids concentration C_V and the standard concentration deviation $C_{V_{std}}$. Identical results were obtained when the recording time was extended to 60 s.

An example of three such time series data is shown in Fig. 4. Curve 1 in Fig. 4a is a typical data record for the case where no particles occurred within the probe. The probe voltage signal was almost constant, showing no fluctuations. Such a data record was obtained from the probe located within the particle-free layer at the vessel top. The maximum signal fluctuations were observed at the interface between the particle-filled layer and the particle-free layer (curve 2 in Fig. 4a). A high decrease of voltage was observed when the bulk of solids reached the measuring volume of the probe. The data record corresponding to fluctuations of the solids concentration within the particle-filled layer is shown in Fig. 4b. Here the calculated average value was significantly lower, i.e. the local particle concentration was higher than that in the cases shown in Fig. 4a. The deviations of particle concentration, $C_{V_{std}}$, were lower than in case of the particle-filled layer interface.

In general, the maximum fluctuations of particle concentration were encountered at the solid/liquid interface, as a result of turbulent flow and the presence of macro-instabilities. Within the dense suspension layer, the solids particle fluctuations were lower and almost constant from the vessel bottom to the solid/liquid interface, as shown in Figs. 5b, 6b, 8 and 10. It should be noted that all our experiments were performed in the steady state, with the particle layer fully developed.

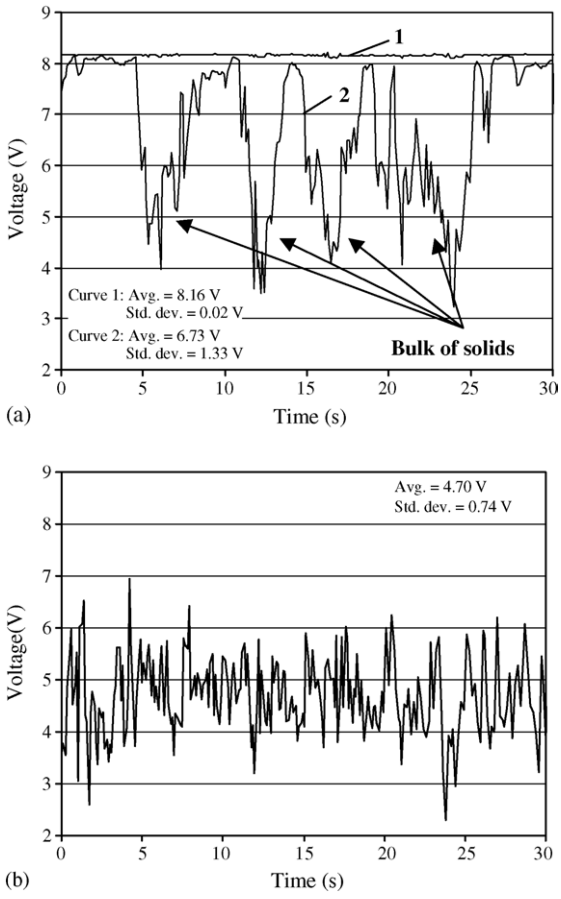

Fig. 4. Probe voltage signals for $d_p = 0.35$ mm, $C_{V_{avg}} = 5$ vol.%, midway plane, $r/R = 0.8$: (a) no solids, $h/H = 0.9$ (curve 1); interface between the clear-liquid layer and the particle-layer, $h/H = 0.8$ (curve 2); (b) within the particle layer, $h/H = 0.2$.

3.2. Particle distribution in the suspension with particle diameter $d_p = 0.35$ mm

The results for suspension with this particle diameter are summarized in Figs. 5–8. Only the results for the vertical plane midway between two baffles (i.e. 45° from the reference baffle plane) are presented here for sake of brevity. Similar results were found for the other investigated planes. A normalized iso-concentration contours $C_V/C_{V_{avg}}$ and a normalized standard deviations $C_{V_{std}}/C_{V_{avg}}$ for the suspensions having $C_{V_{avg}} = 5$ and 10 vol.% (off-bottom clearance $H_2 = d$) are shown in Figs. 5 and 6. These dependences clearly indicate the existence of a particle layer whose height fluctuated approximately in the range of $h/H = 0.65$–0.85 for $C_{V_{avg}} = 5$ vol.% (Fig. 5) and in the range of $h/H = 0.60$–0.80 for $C_{V_{avg}} = 10$ vol.% (Fig. 6). As discussed in previous section, in this region the normalized concentration deviations reached the maximum.

On the contrary, the concentration fluctuations were small between the vessel bottom and the height $h/H = 0.5$ for $C_{V_{avg}} = 5$ vol.% (Fig. 5) and $h/H = 0.6$ for $C_{V_{avg}} = 10$ vol.% (Fig. 6). In this region, the suspension layer observed was "fully developed" and the normalized concentration deviations were in the range of $C_{V_{std}}/C_{V_{avg}} = 0.15$–0.3. It may be inferred that a well-ordered flow pattern was established within the parti-

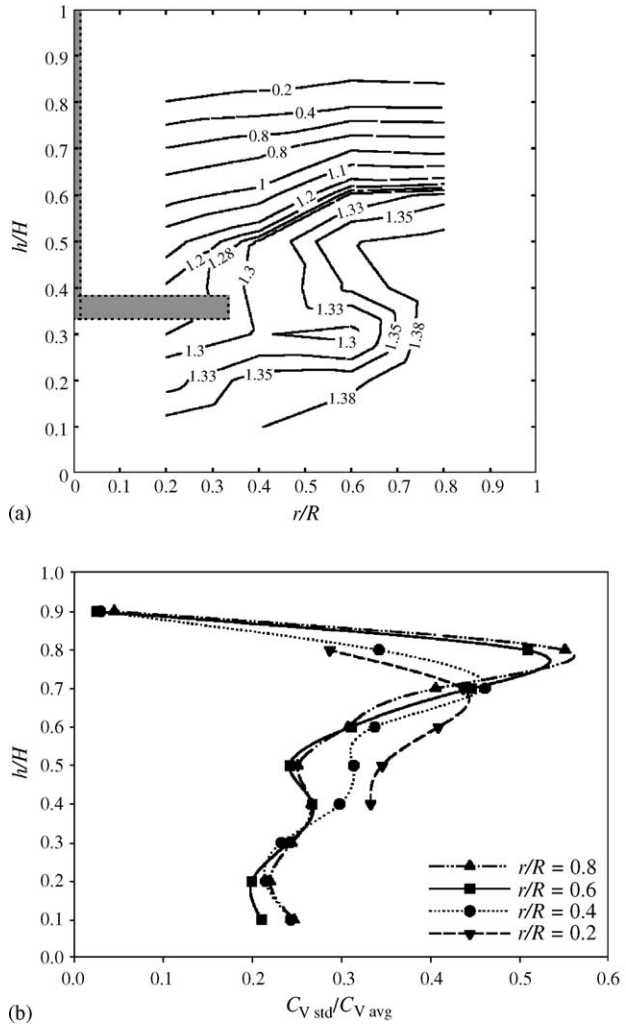

Fig. 5. Normalized particle concentration map $C_V/C_{V_{avg}}$ (a) and corresponding standard deviations $C_{V_{std}}/C_{V_{avg}}$ (b); midway plane, $C_{V_{avg}} = 5$ vol.%, $H_2/d = 1$, $d_p = 0.35$ mm.

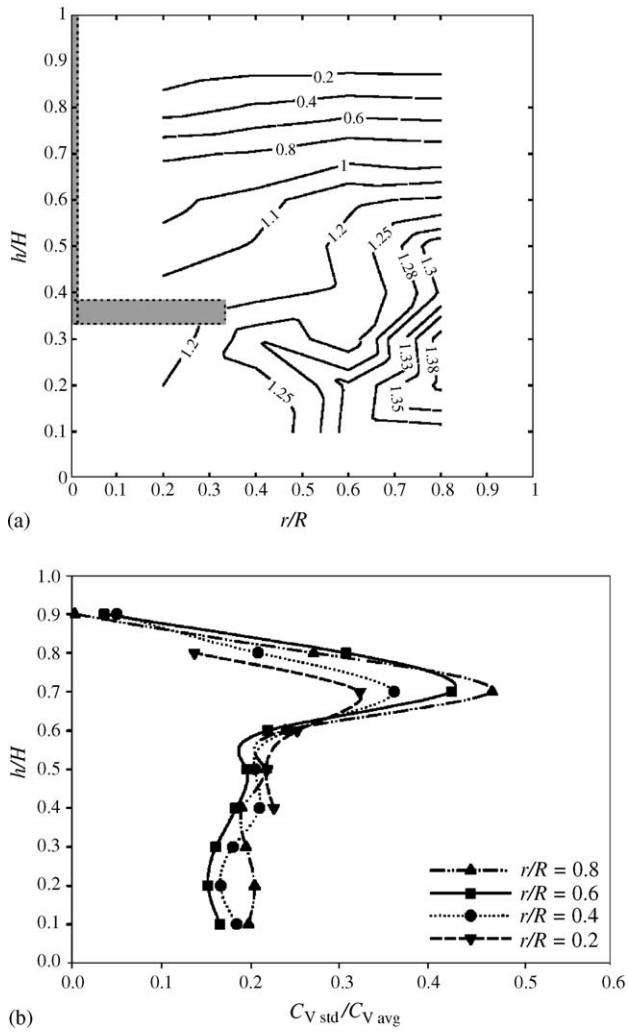

Fig. 6. Normalized particle concentration map $C_V/C_{V_{avg}}$ (a) and corresponding standard deviations $C_{V_{std}}/C_{V_{avg}}$ (b); midway plane, $C_{V_{avg}} = 10$ vol.%, $H_2/d = 1$, $d_p = 0.35$ mm.

cle layer and a "compression action" was exerted on the fluid flow pattern. The circulation loops generated by the impeller were confined to the region containing the solids, while the clear liquid layer near the liquid surface was almost still. This is in agreement with our experimental evidence that the clear liquid layer near the liquid surface was almost still, especially in the experiments conducted at higher solid concentration and lower impeller off-bottom clearance. This phenomenon corresponds with the computational results by Micale et al. [31].

The normalised axial concentration profiles $C_V/C_{V_{avg}}$ for the two solid concentrations and two impeller off-bottom clearances studied are rendered in Fig. 7a and b. Indeed, the lower height of the suspension layer corresponded with increasing average solid concentration and decreasing impeller off-bottom clearance. This is in agreement with earlier results [25,30,31]. This conclusion can also be derived from Fig. 8 where the absolute standard concentration deviations $C_{V_{std}}$ are plotted against the relative heights h/H. The same results were obtained for the suspension with particle diameter $d_p = 0.14$ mm, see Fig. 10.

The local concentration values, C_V, were low in the region above the impeller ($r/R = 0.2$) and the radial concentration profile was found, see Figs. 5a and 6a. Further discussion relating to the radial concentration gradient can be found in Section 3.5. The height of the interface between the clear-liquid layer and the suspension layer was lower in the region above the impeller, and was not well defined. Although the values of $C_{V_{std}}/C_{V_{avg}}$ for $r/R = 0.2$ attained a maximum at the interface, they were the lowest of all the maxima attained in the positions $r/R = 0.4$, 0.6 and 0.8, as shown in Figs. 5b and 6b. The same conclusion was found to apply to a suspension involving smaller particles (data not shown).

Finally, it should be noted that the interface between the clear liquid and the suspension layer became sharper and more clearly defined as the solid concentration was increased.

3.3. Particle distribution in the suspension with particle diameter $d_p = 0.14$ mm

The graphic representations for the suspension involving the particle diameter $d_p = 0.14$ mm are shown in Figs. 9 and 10. Similar results and conclusions presented in Section 3.2 were

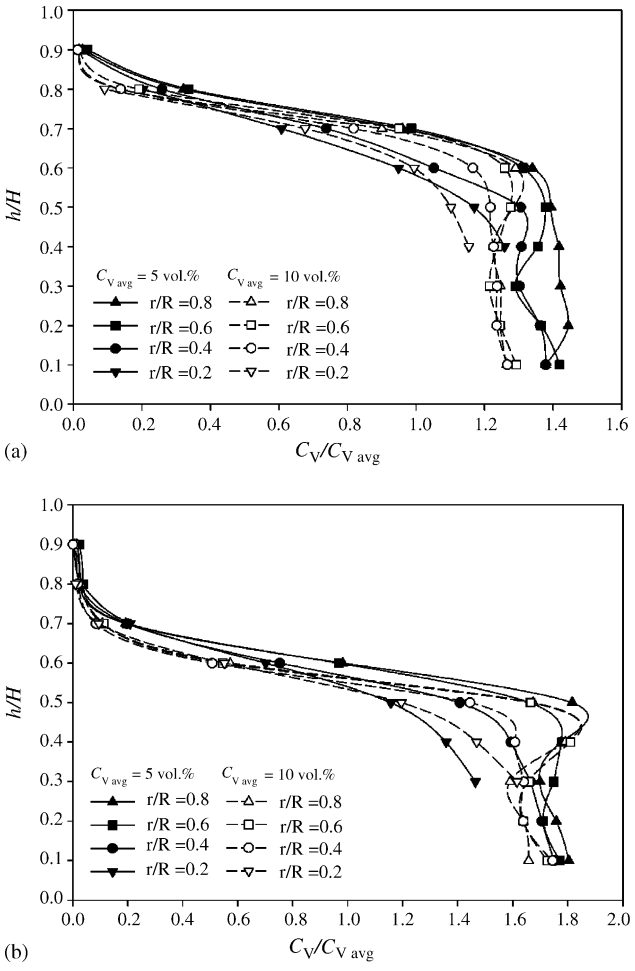

Fig. 7. Normalized axial concentration profiles $C_V/C_{V_{avg}}$ for different impeller positions $H_2/d = 1$ (a), $H_2/d = 0.5$ (b); $d_p = 0.35$ mm, midway plane.

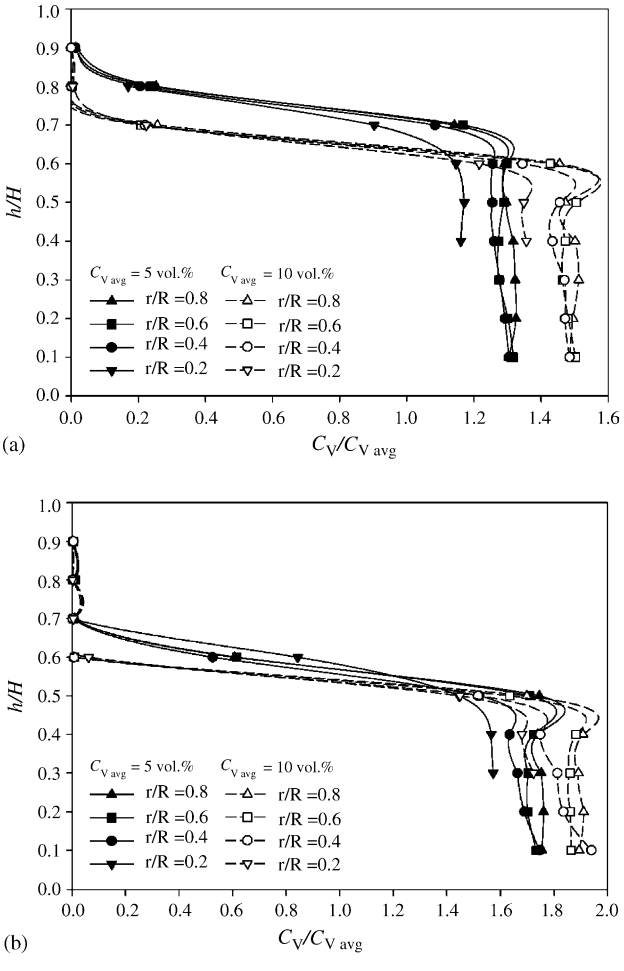

Fig. 9. Normalized axial concentration profiles $C_V/C_{V_{avg}}$ for different impeller positions $H_2/d = 1$ (a), $H_2/d = 0.5$ (b); $d_p = 0.14$ mm, midway plane.

obtained. The normalized axial concentration profiles for both solid concentrations and both off-bottom clearances are rendered in Fig. 9. The absolute particle concentration deviations $C_{V_{std}}$ for radial position $r/R = 0.8$ are shown in Fig. 10. The highest cloud height was observed in the experiment with $C_{V_{avg}} = 5$ vol.% and $H_2/d = 1$ (see Fig. 10). On the contrary, the lowest cloud height was observed for the suspension having $C_{V_{avg}} = 10$ vol.% at an impeller off-bottom clearance $H_2/d = 0.5$.

Unlike the suspension with larger particles, an almost uniform concentration distribution was found to persist in the axial

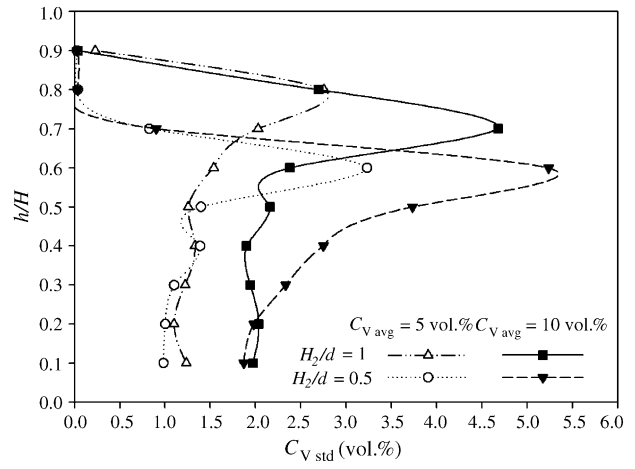

Fig. 8. Variation of standard concentration deviations $C_{V_{std}}$ at different vessel heights h/H; $d_p = 0.35$ mm, midway plane, $r/R = 0.8$.

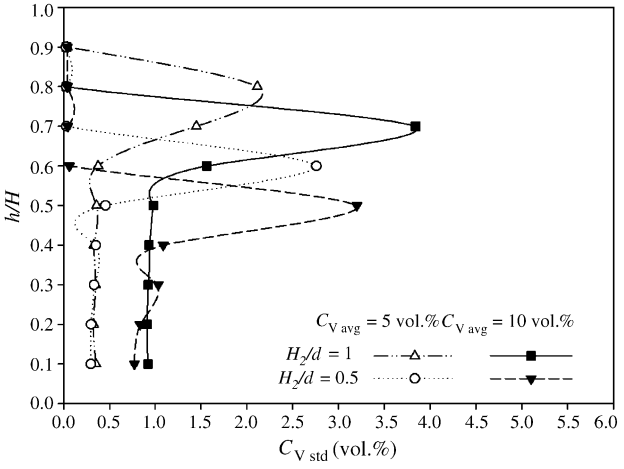

Fig. 10. Variation of standard concentration deviations $C_{V_{std}}$ at different vessel heights h/H; $d_p = 0.14$ mm, midway plane, $r/R = 0.8$.

direction within the "fully-developed" particle layer, as shown in Fig. 9. Within the limits of experimental error, the suspension layer appeared to be more homogeneous than that for the suspension with larger particles, although in the region above the impeller ($r/R = 0.2$) the solids concentrations were lower again. The reader is referred to Section 3.5 for a discussion of the radial concentration gradients.

Even if the maximum concentration fluctuations were found at the solid/liquid interface, while within the particle layer they were significantly lower and more uniform (Fig. 10), it holds in general that the concentration fluctuations were lower for all axial positions tested, in contrast to the suspension of particles having a diameter $d_p = 0.35$ mm, see Figs. 8 and 10. This could probably be caused by lower critical impeller speeds, n_{js}, and consequently, by smaller turbulent fluctuations.

3.4. Accuracy of measurement and data verification

The accuracy of the concentration profiles of solids was ±0.2 vol.% in the region of the "fully developed" suspension layer, even though the standard concentration deviations, $C_{V_{std}}$, were in the range from 0.3 to 2 vol.%. At the particle layer interface, where the fluctuations were maximum, the accuracy of determination of the solids concentration was ±0.5 vol.% and the deviations, $C_{V_{std}}$, were within the range of 2–5.5 vol.%. The accuracy of measurements was significantly increased by replication of the experiments.

The correctness of the experimentally established distribution of particle concentrations was verified by mass balance computations of solid phase. The average axial concentrations $C_{V_{avg\ axial}}$ for each radial position r/R on a given measuring plane were calculated according to Eq. 4:

$$C_{V_{avg\ \ axial}} = \frac{1}{(h/H)_{max} - (h/H)_{min}} \times \int_{(h/H)_{min}}^{(h/H)_{max}} C_V (h/H)_i \, d(h/H) \quad (4)$$

in the range of experimental relative heights $(h/H)_{max} = 0.9$ and $(h/H)_{min} = 0.1$ using trapezoidal integration. The plane location within one vessel quadrant was regular for the reference baffle plane and then at 30° and 60° from the baffle plane. Then, the average solids concentration was calculated as an arithmetical mean of the $C_{V_{avg\,axial}}$ values obtained for the radial positions r/R examined in these three planes. The average axial concentrations $C_{V_{avg\,axial}}$ corresponding to the midway plane were not used for the calculation of the average concentration $C_{V_{avg}}$, in order to exclude potentially different statistical weights of each plane due to various angle differences between the planes. The calculated average particle concentrations thus obtained were within the ranges of 5.01–5.20 vol.% (for $C_{V_{avg}} = 5$ vol.%) and of 9.95–10.19 vol.% (for $C_{V_{avg}} = 10$ vol.%), for all the conditions tested. The agreement was very good, but it is worth noting that the region under the impeller was not measured, and the concentrations at these points (which were used for numerical integration) were extrapolated from the experimental concentrations obtained at the closest neighbouring points. These concentrations were also used to examine the radial gradients and to plot the normalised concentration maps in Figs. 5a and 6a. The mean particle concentrations for the midway plane 45° were in the ranges from 5.11 to 5.24 vol.% (for $C_{V_{avg}} = 5$ vol.%) and from 9.61 to 10.20 vol.% (for $C_{V_{avg}} = 10$ vol.%), calculated as an arithmetic mean of the average axial concentrations $C_{V_{avg\,axial}}$ belonging to this plane. This result shows that the alternative of including the data for this plane in the computation of the mean particle concentration, together with data for other regularly located planes, does not generate any significant differences.

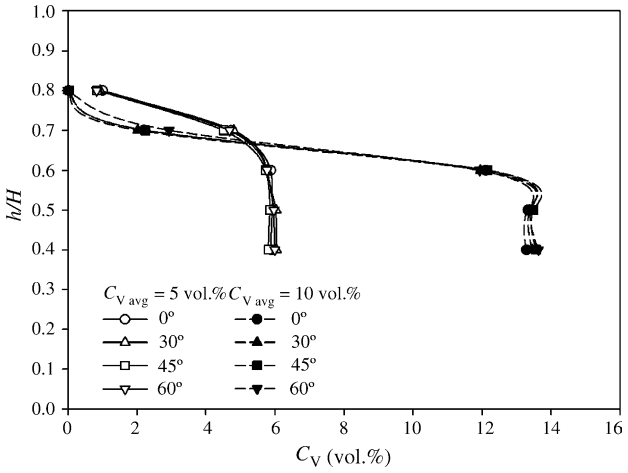

Fig. 11. Axial concentration profiles close to the vessel axis ($r/R = 0.2$), $H_2/d = 1$, $d_p = 0.14$ mm.

Finally, it can be assumed that in the region near the vessel axis ($r/R = 0.2$) the fluid flow is tangentially symmetrical and not much affected by presence of baffles. The experimental points (3, 7, 11, 15 in Fig. 3) were not far from each other, as against the point-to-point distances in the tangential planes $r/R = 0.6$ and 0.8. In this region, the axial concentration profiles for $r/R = 0.2$ ought to be comparable. In this respect, a good agreement was found as well, as shown in Fig. 11, and the same results were found for all the experimental conditions investigated. Finally, it could be noted that the fluid flow near the vessel wall is to some extent influenced by baffles and, therefore, different concentration profiles were found in front of and behind the baffle (data not shown).

3.5. Radial particle distribution

The average axial concentrations $C_{V_{avg\,axial}}$ plotted as a function of the radial positions r/R can be found in Fig. 12a and b. A practically linear increase of radial concentrations was observed for both suspensions with different particle diameters at $C_{V_{avg}} = 5$ vol.% in the range of $r/R = 0.2$–0.6, see Fig. 12a. In this region, it can be assumed that the influence of baffles on the flow pattern is significantly lower than in the range of $r/R = 0.6$–1; therefore, the $C_{V_{avg\,axial}}$ values obtained in different tangential positions can be summarised with a satisfactory accuracy for linear regression. In the range of $r/R = 0.6$–1, the average axial concentrations $C_{V_{avg\,axial}}$ may already have different statistical weights in the tangential direction due to the baffle effects.

Table 3
Straight line parameters A, B of radial concentration gradients in the range of $r/R = 0.2–0.6$

H_2/d	Linear regression $C_{V_{avg\,axial}} = A(r/R) + B$ for $r/R = 0.2–0.6$											
	$d_p = 0.14$ mm						$d_p = 0.144$ mm					
	$C_{V_{avg}} = 5$ vol.%			$C_{V_{avg}} = 10$ vol.%			$C_{V_{avg}} = 5$ vol.%			$C_{V_{avg}} = 10$ vol.%		
	A	B	$\Delta C_{V_{avg\,axial}}$ (%)[a]	A	B	$\Delta C_{V_{avg\,axial}}$ (%)[a]	A	B	$\Delta C_{V_{avg\,axial}}$ (%)[a]	A	B	$\Delta C_{V_{avg\,axial}}$ (%)[a]
1	1.16	4.69	9.2	2.07	9.27	8.3	2.10	4.10	16.7	2.60	8.76	10.4
0.5	0.91	4.69	7.2	1.87	9.17	7.5	2.96	3.87	23.7	3.25	8.59	13.0

[a] Percentage concentration increase in radial direction for $r/R = 0.2–0.6$.

As the solids concentration increased up to $C_{V_{avg}} = 10$ vol.%, the particle-filled layer became concentrated and more homogeneous in the region near the vessel wall. For $r/R = 0.2–0.6$ again, a linearly rising concentration was found, whereas the concentration became almost constant at $r/R = 0.6–0.8$, see Fig. 12b.

Even though the results presented in Fig. 12a and b apply to a higher impeller off-bottom clearance $H_2 = d$, the same conclusions were obtained for a lower impeller position, $H_2/d = 0.5$. The straight-line parameters (A, B) characterizing the radial concentration gradients are summarized in Table 3.

For the suspension involving the particle diameter $d_p = 0.35$ mm, the concentration increase from the vessel axis to the vessel wall in the region $r/R = 0.2–0.6$ is lower when the average solids concentration is increased. At $C_{V_{avg}} = 5$ vol.% and $H_2 = d$ the concentration increase is nearly 17%, compared to 10.4% at $C_{V_{avg}} = 10$ vol.%. The suspension with $C_{V_{avg}} = 10$ vol.% was more homogeneous.

Similar results were obtained for the suspension involving the particle diameter $d_p = 0.14$ mm. The radial concentration gradient was observed for all experimental conditions, but the differences between the concentration gradients for $C_{V_{avg}} = 5$ and 10 vol.% became smaller. At the impeller off-bottom clearance $H_2/d = 0.5$ there was almost no difference in concentration gradient with increasing average solids concentration, see Table 3.

In general, the higher was the solids concentration $C_{V_{avg}}$ and the smaller were the solid particles, the more homogeneous was the suspension obtained. In the case of the suspension with particle diameter $d_p = 0.14$ mm, the increase of the average particle concentration did not result in any significant increase of homogeneity of the suspension.

Finally, it can be assumed that due to the elliptical circulation flow, which is typical for axial-flow impellers, the particle concentration was lower above the impeller. These findings about the existence of a radial gradient are in agreement with other papers [34,35], which also refer to pitched blade turbines.

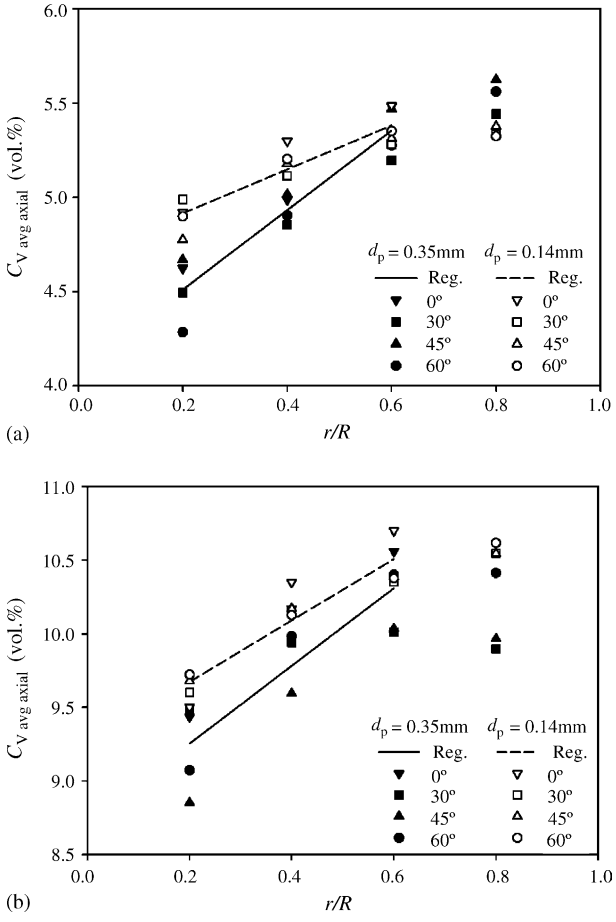

Fig. 12. The average radial concentration profiles for $C_{V_{avg}} = 5$ vol.% (a) and $C_{V_{avg}} = 10$ vol.% (b), $H_2/d = 1$.

4. Conclusions

The particle distributions in stirred solid/liquid systems were determined for eight experimental conditions, all of them corresponding to the state of complete suspension. The experimental results highlight the presence of an interface between the clear liquid layer (the particle-free layer) and the suspension layer.

The maximum concentration fluctuations were observed at the suspension layer interface. On the other hand, the fluctuations were significantly lower and almost uniform within the "fully developed" suspension layer. The height of the suspension layer was reduced by increasing the average solids concentration and decreasing the impeller off-bottom clearance. The presence of a radial concentration gradient was observed for all the experimental conditions examined. The higher was the mean solids concentration $C_{V_{avg}}$ and the smaller were the solid particles, the more homogeneous was the suspension obtained.

On the whole, these results offer new information conducive to the understanding of the solid–liquid mixing processes. Especially, they explore the degree of homogeneity of the suspension

layer and attempt to quantify the existence of the radial concentration gradient. It is hoped that the present results may be considered to provide a useful groundwork for CFD modelling of moderately concentrated suspensions. It should also be noted that some of these results were used for testing CFD simulation capabilities [41], yielding good predictions of particle distribution which were in line with experimental data.

Acknowledgements

The authors are grateful to Assoc. Prof. Ivan Fořt for his valuable advice, interest and comments. Support by Czech Grant Agency (Grant No. 104/03/H141) and by Czech Ministry of Education (Project No. MSM6046137306) is acknowledged.

References

[1] Th.N. Zwietering, Chem. Eng. Sci. 8 (1958) 244–253.
[2] F. Magelli, D. Fajner, M. Nocentini, G. Pasquali, Chem. Eng. Sci. 45 (1990) 615–625.
[3] F. Magelli, D. Fajner, M. Nocentini, G. Pasquali, V. Marisko, P. Ditl, Chem. Eng. Process. 29 (1991) 27–32.
[4] P.A. Shamlou, E. Koutsakos, Chem. Eng. Sci. 44 (1989) 529–542.
[5] R.S. MacTaggart, H.A. Nasr-El-Din, J.H. Masliyah, Chem. Eng. Sci. 48 (1993) 921–931.
[6] A.A. Barresi, G. Baldi, Chem. Eng. Sci. 42 (1987) 2949–2956.
[7] A.A. Barresi, G. Baldi, Chem. Eng. Sci. 42 (1987) 2969–2972.
[8] A.A. Barresi, N. Kuzmanic', G. Baldi, IChemE. Symp. Ser. 136 (1994) 17–24.
[9] J.M. Smith, Trans. IChemE. 68 (1990) 3–6.
[10] L. Musil, J. Vlk, Chem. Eng. Sci. 33 (1978) 1123–1131.
[11] V. Machoň, I. Fořt, J. Skřivánek, Proceedings of the Fourth European Conference on Mixing, Leeuwenhorst, The Netherlands, 1982, pp. 289–302.
[12] F. Rieger, P. Ditl, O. Havelková, Proceedings of the Sixth European Conference on Mixing, Pavia, Italy, 1988, pp. 251–258.
[13] P. Bílek, F. Rieger, Collect. Czech. Chem. Commun. 55 (1990) 2169–2181.
[14] A.T.C. Mak, S.W. Ruszkowski, IChemE. Symp. Ser. 121 (1990) 379–395.
[15] M. Micheletti, L. Nikiforaki, K.C. Lee, M. Yianneskis, Ind. Eng. Chem. Res. 42 (2003) 6236–6249.
[16] M. Špidla, V. Sinevič, M. Jahoda, V. Machoň, Proceedings of the 31th International Conference on SSCHE, Tatranské Matliare, Slovak Republic, 2004, pp. 1–10, P.091.
[17] D.M. Considine, G.D. Considine, Process Instruments and Controls Handbook, 3rd ed., McGraw-Hill, New York, 1985.
[18] H.A. Nasr-El-Din, C.A. Shook, J. Colwell, Int. J. Multiphase Flow 13 (1987) 365–378.
[19] R.S. MacTaggart, H.A. Nasr-El-Din, J.H. Masliyah, Sep. Technol. 3 (1993) 151–160.
[20] H.A. Nasr-El-Din, R.S. MacTaggart, J.H. Masliyah, Chem. Eng. Sci. 51 (1996) 1209–1220.
[21] L. Musil, Chem. Eng. Sci. 39 (1984) 629–636.
[22] C. Buurman, G. Resoort, A. Plaschkes, Chem. Eng. Sci. 41 (1986) 2865–2871.
[23] M.T. Hicks, K.J. Myers, A. Bakker, Chem. Eng. Com. 160 (1997) 137–155.
[24] W. Bujalski, K. Takenaka, S. Paolini, M. Jahoda, A. Paglianti, K. Takahashi, A.W. Nienow, A.W. Etchells, Trans. IChemE. Part A, Chem. Eng. Res. Des. 77 (1999) 241–247.
[25] A.A. Barresi, G. Baldi, Proceedings of the 10th European Conference on Mixing, Delft, The Netherlands, 2000, pp. 133–140.
[26] K. Takenaka, G. Ciervo, D. Monti, W. Bujalski, A.W. Etchells, A.W. Nienow, J. Chem. Eng. Japan 34 (2001) 606–612.
[27] A. Brucato, G. Micale, G. Montante, A. Scuzzarella, Proceedings of the 10th Workshop on Two-Phase Flow Prediction, Merseburg, Germany, 2002, pp. 255–264.
[28] G. Micale, A. Scuzzarella, P. Lettieri, F. Grisafi, A. Brucato, Proceedings of the 8th Int. Conf. Multiphase Flow in Industrial plants, Alba, Italia, 2002, pp. 468–484.
[29] K.J. Bittorf, S.M. Kresta, Trans. IChemE. Part A, Chem. Eng. Res. Des. 81 (2003) 568–577.
[30] M. Špidla, G. Micale, F. Grisafi, A. Brucato, V. Machoň, Proceedings of the 16th Internat. Congress CHISA, Prague, Czech Republic, 2004, pp. 1–10, P5.177.
[31] G. Micale, F. Grisafi, L. Rizzuti, A. Brucato, Trans. IChemE. Part A, Chem. Eng. Res. Des. 82 (2004) 1204–1213.
[32] H. Yamazaki, K. Tojo, K. Miyanami, Powder Technol. 48 (1986) 205–216.
[33] G. Montante, D. Pinelli, F. Magelli, Can. J. Chem. Eng. 80 (2002) 665–673.
[34] R. Angst, M. Kraume, Proceedings of the Third International Symposium on Two-Phase Flow Modelling and Experimentation, Pisa, Italy, 2004, ISBN 88-467-1075-4.
[35] R. Angst, M. Kraume, Proceedings of the 11th Workshop on Two-Phase Flow Prediction, Merseburg, Germany, 2005, ISBN 3-86010-767-4.
[36] F. Rieger, P. Ditl, Chem. Eng. Sci. 49 (1994) 2219–2227.
[37] F. Rieger, Reports of the Faculty of Chemical and Process Engineering, vol. XXV, no. 1–3, Warsaw University of Technology, 1999, pp. 211–214.
[38] F. Rieger, Chem. Eng. J. 79 (2000) 171–175.
[39] F. Rieger, Chem. Eng. Process. 41 (2002) 381–384.
[40] F. Rieger, T. Jirout, P. Ditl, B. Kysela, R. Sperling, S. Jembere, Proceedings of the 11th European Conference on Mixing, Bamberg, Germany, 2003, pp. 503–509.
[41] M. Špidla, M. Moštěk, V. Sinevič, M. Jahoda, V. Machoň, Proceedings of the 32th International Conference on SSCHE, Tatranské Matliare, Slovak Republic, 2005, pp. 1–11, P.127.